Science of the Total Environment 710 (2020) 135620

Contents lists available at ScienceDirect

Science of the Total Environment

journal homepage: www.elsevier.com/locate/scitotenv

Source apportionment and regional transport of anthropogenic secondary organic aerosol during winter pollution periods in the Yangtze River Delta, China

Jie Liu [a], Juanyong Shen [a], Zhen Cheng [a,*], Peng Wang [b,*], Qi Ying [c], Qianbiao Zhao [d], Yihua Zhang [d], Yue Zhao [a], Qingyan Fu [d]

[a] School of Environmental Science and Engineering, Shanghai Jiao Tong University, Shanghai 200240, China
[b] Department of Civil and Environmental Engineering, The Hong Kong Polytechnic University, 999077, Hong Kong, China
[c] Zachry Department of Civil Engineering, Texas A&M University, College Station, TX 77843, USA
[d] Shanghai Environmental Monitoring Center, Shanghai 200235, China

HIGHLIGHTS

- Formation path and source region contributions to SOA in the YRD region were investigated.
- Industry source in the YRD region dominates total SOA during the heavy polluted episodes.
- Reginal control policy should be considered in the VOCs and SOA reduction in YRD.

GRAPHICAL ABSTRACT

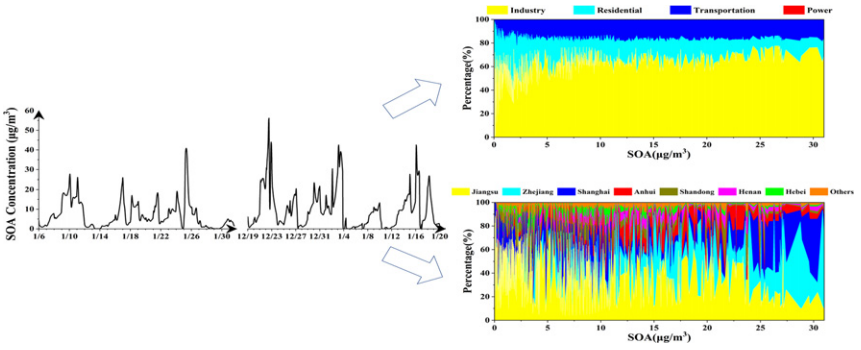

ARTICLE INFO

Article history:
Received 13 September 2019
Received in revised form 17 November 2019
Accepted 17 November 2019
Available online 23 November 2019

Editor: Pingqing Fu

Keywords:
Source apportionment
Regional transport
Secondary organic aerosol
Heavy pollution episodes
Fine particulate

ABSTRACT

Since the concentrations of primary particles and secondary inorganic aerosol components have been reduced significantly due to stringent emission controls, quantifying the source contributions and regional transport of secondary organic aerosol (SOA) is critical to further improve air quality in eastern China. In this study, the Community Multiscale Air Quality (CMAQ) model coupled with the updated SAPRC-11 photochemical mechanism and a revised SOA module was applied to investigate the emission sector and regional contributions to SOA in winter 2015 (January 5–26, 2015) and 2016 (December 20, 2015–January 20, 2016) in the Yangtze River Delta (YRD). The model is generally capable of reproducing the observed SOA concentrations at the Qingpu Supersite in Shanghai. The observed and predicted SOA concentrations are 6.4 μg/m^3 and 6.9 μg/m^3 in winter 2015, and 5.7 μg/m^3 and 9.6 μg/m^3 in winter 2016. The mean fraction bias (MFB) of the hourly SOA predictions is 0.22 and 0.32, respectively. High SOA concentrations in the wintertime of YRD are mainly due to aromatic compounds and dicarbonyls (glyoxal and methylglyoxal), which, on average, account for 43% and 53% of total SOA, respectively. The average contributions of industrial, residential, and transportation sectors in the YRD region during the entire simulation periods are 61%, 22%, and 17%, respectively. At the Qingpu Supersite in Shanghai, the industrial sector contributes to as much as 65% of total SOA in the heavy pollution episode of 2016. The contributions from transportation and residential sectors are 16% and 17%, respectively, during the same episode. The industry

* Corresponding authors.
E-mail addresses: chengz88@sjtu.edu.cn (Z. Cheng), peng.ce.wang@polyu.edu.hk (P. Wang).

https://doi.org/10.1016/j.scitotenv.2019.135620

emissions from the Jiangsu, Zhejiang, and Shanghai are major contributors to the SOA at the Qingpu supersite during the heavy-polluted episodes, accounting for 31%, 19%, and 14% of the total predicted SOA. This study represents the first detailed regional modeling study of source region contributions to SOA in the YRD region and the detailed analyses of SOA in two winters months complement the previous SOA source apportionment studies focusing on seasonal average contributions.

1. Introduction

Although the annual average concentrations of $PM_{2.5}$ in China have been reduced by 33.3% from 2013 to 2017 (Huang et al., 2018), regional heavy $PM_{2.5}$ pollution events still occur frequently during autumn and winter seasons (Wei et al., 2019). Organic aerosols (OA) are an important contributor to the mass of fine particulate matter ($PM_{2.5}$) (Crippa et al., 2014; Jimenez et al., 2009). Secondary organic aerosol (SOA), formed from both anthropogenic and biogenic oxidation products of volatile and semi-volatile species, could account for over half of the total OA (Jimenez et al., 2009). While the emissions of primary particles, sulfur dioxide and nitrogen oxides have been reduced significantly in recent years, of the emissions of volatile organic compounds (VOCs), some of which are important precursors of SOA, remained relatively unchanged (Li et al., 2019). Hence, quantifying the source apportionment and regional transportation of SOA is critical for implementing efficient mitigation measures of heavy pollution events.

A few studies related to source apportionment of SOA in China have been reported. Zhu et al. (2017) used a secondary organic tracer approach (Kleindienst et al., 2007) and the positive matrix factorization (PMF) to examine the sources of anthropogenic and biogenic SOA at Mt. Tai in Shandong province. Lin et al. (2016) investigated the local and distant source contributions to SOA in Beijing in the summertime through the Comprehensive Air Quality Model with Extensions (CAMx) along with the volatility basis-set (VBS) approach to model SOA. Jiang et al. (2012) used the Weather Research and Forecasting (WRF) model coupled with Chemistry (WRF/Chem), coupled with a secondary organic aerosol model (SORGAM), to determine the relative contributions of anthropogenic and biogenic sources to SOA in 2006 over China. Hu et al. (2017b) and Wang et al. (2018) used the Community Multiscale Air Quality (CMAQ) model v5.0.1 with a revised SOA module (Ying et al., 2015) to improve SOA predictions and source apportionment in 2013 over whole China. However, the previous modeling studies were mainly focused on the season average or during the summer times. Little attention has been drawn for SOA during winter pollution episodes, especially for the mega-city clusters such as the Yangtze River Delta (YRD). Liu et al. (2018) and Wu et al. (2019) found that the emissions of biogenic organic compounds are comparatively low in the YRD due to the dieback of vegetation and the presence of snow cover in winter, which cause the leaf area index to decrease sharply. While this suggests that biogenic contributions to SOA might be low in the YRD region in winter, it is unclear how much SOA will be produced due to anthropogenic emission and how regional transport can contribute to SOA concentrations, especially during winter heavy pollution episodes in the YRD.

The aim of this study is to investigate the SOA formation, transport and source contributions during high winter pollution periods in the YRD using a three-dimensional source-oriented chemical transport model. The capability of the model in reproducing the evolution of SOA during two months in the winter of 2015 and 2016 is evaluated by comparing it with field measurements. The emission sector and source region contributions are quantified. The results of this study are expected to provide a comprehensive understanding of the SOA formation processes, the major precursors, and the source and regional contributions to SOA during winter polluted episodes. This information can provide direct support for the development of emission control strategies in the YRD region.

2. Materials and methodology

2.1. Model configurations

The air quality simulation in this study covered two winter months in two different years, January 5–26, 2015 (winter 2015) and December 19, 2015 to January 20, 2016 (winter 2016). Three heavy pollution episodes (EP1: January 7–12, 2015; EP2: January 20–26, 2015; EP3: December 28, 2015–January 5, 2016), and one clean episode (EP4: January 11–12, 2016) were identified and selected for further analysis. The modeling domain is 36×36 km^2 in horizontal resolution and covers China and its surrounding countries in east and southeast Asia (Fig. 1a). The meteorological data were derived from the results of the WRF model v3.9 with initial and boundary conditions from the global

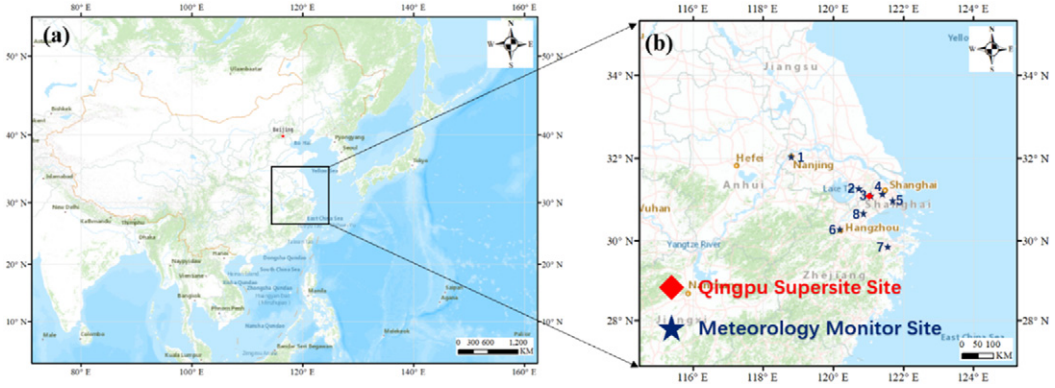

Fig. 1. (a) The model (WRF-CMAQ) domain covers China and (b) the Yangtze River Delta (YRD) region focused in this study. This area covers 210×140 grid cells. The blue star represents the monitor site in the YRD. The red rhombus represents the Qingpu Supersite.

reanalysis data from the National Centers for Environmental Prediction (NCEP) (https://rda.ucar.edu/). A detailed evaluation of the meteorological predictions is described in Section 3.1. The CMAQ model v5.0.1 (Byun and Schere, 2006) with modifications to improve the SOA simulation was used in this study. Gaseous chemical mechanism used in this study is a lumped version of SAPRC-11 (Carter and Heo, 2013) and the SOA module in the AERO6 aerosol mechanism was modified to include reactive surface uptake of dicarbonyls and isoprene epoxides, which are shown to improve SOA predictions in the eastern United States (Ying et al., 2015). Other changes in the SOA module, including the updated aerosol yields to account for vapor wall loss during chamber experiments, have been described elsewhere (Hu et al., 2016, 2017a, 2017b) and thus are not repeated here. Initial and boundary conditions for the CMAQ simulations were based on the vertical distributions of concentrations, which represent clean continental conditions. The first 5 days of the simulation were excluded to avoid the impact of initial conditions. The source tracking approach for SOA in the CTM has been described by Zhang and Ying (2011b). Implementation of the approach in CMAQ can be found in Ying et al. (2015) and Wang et al. (2018). A brief description of this technique is included in Section 2.2.

The anthropogenic emission inventory is based on the Multi-resolution Emission Inventory for China (MEIC 2016) (http://www.meicmodel.org/), which has a resolution of 0.25°×0.25°. Biogenic emissions are not included in this study due to its negligible influence on SOA contributions in the winter (Hu et al., 2017b; Kang et al., 2018; Wang et al., 2018).

2.2. Source-oriented method for SOA

Ying and Krishnan (2010) and Zhang and Ying (2011a) developed the source-oriented method in CMAQ to determine the contribution of organic compounds and nitrogen oxides to ozone formation in Texas. It is subsequently used to study the contributions to secondary nitrate, sulfate and ammonium (Zhang et al., 2012) and SOA (Wang et al., 2018) in China.

A brief introduction of this source-oriented method of SOA is described in the following. Taking the model species ARO2 (more reactive aromatics with $k_{OH} > 5 \times 10^{-4}$ ppm^{-1} min^{-1}) as an example, to explicitly track SOA formation from a specific source X, the ARO2 reaction with OH and the subsequent reaction of the peroxy radical with HO_2 are expanded into two sets of reactions, as shown in reaction sets R1a and R1b:

$$ARO2^X + OH \rightarrow ARO2RO2^X + HO_2 \rightarrow XYLHRXN^X + \ldots$$

$$ARO2 + OH \rightarrow ARO2RO2 + HO_2 \rightarrow XYLHRXN + \ldots \quad \text{(R1b)}$$

The superscript X on ARO2 in reaction set (R1a) is used to represent the aromatic compounds from a specified source X (for example, aromatics from power plants in Shanghai or aromatics from industrial emissions in Jiangsu), while the none-tagged ARO2 in R1b represents the aromatics emitted from all the other sources. For the tagged emission $ARO2^X$, the source-tagged reaction counter species $XYLHRXN^X$ is used to track the amount of $ARO2^X$ reacted in each chemistry timestep that can form semi-volatile products under the low NOx condition. Subsequently, the amounts of semi-volatile products that can form SOA based on the two-product model (SV_XYL1^X and SV_XYL2^X) are updated in the SOA module based on $XYLHRXN^X$ and fine mode SOA based-on the gas-to-particle partitioning of the two semi-volatile products ($AXYL1J^X$ and $AXYL2J^X$) are determined. For the non-tagged ARO2, which represents the emissions from all other sources, the total amounts of SOA from these emissions (AXYL1J and AXYL2J) are determined using the same approach. One explicit source (from a single sector of the single region) was tracked in a single simulation to make sure the overall reactivity of the system. To determine the source contribution for M explicit sources and N explicit regions, a total of M × N regional simulations are conducted in this study.

2.3. Ambient observation datasets

Hourly mass concentrations of organic carbon (OC) and elemental carbon (EC) were measured by a field semi-continuous OC/EC analyzer (RT-4, Sunset Lab, USA) with 30-minute resolution (Bae et al., 2004) at a

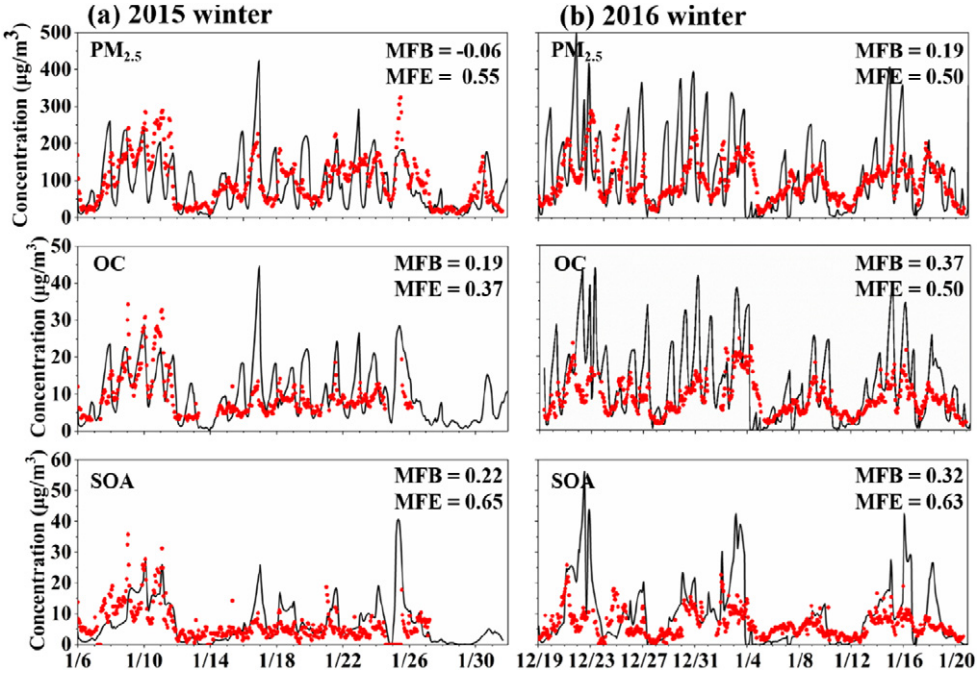

Fig. 2. $PM_{2.5}$, OC and SOA temporal variation at Qingpu supersite of (a) 2015 winter and (b) 2016 winter. The black line represents the predicted data using SAPRC11 mechanism and revised SOA module. Red dots represent the observed data (SOA is calculated by $(EC/OC)_{min}$ method).

regional supersite (120.98°E, 31.09°N) in the Qingpu District of Shanghai, the geographical center of the YRD region (shown in Fig. 1b). The regional supersite is located on the rooftop of the Environmental Monitoring Building (about 20 m above the ground). Secondary organic carbon (SOC) was then estimated according to the minimum OC/EC ratio method (Cao et al., 2004; Castro et al., 1999). Fig. S1 illustrates the observed OC, EC concentrations and OC/EC ratio of 2015 winter and 2016 winter at the Qingpu Supersite. The $(OC/EC)_{min}$ was assigned to 1.0 for the winter of 2015 and 1.3 for the winter of 2016 according to the regressions of all data points of OC versus EC for each month. The OM/OC ratio for the SOA was set to 1.8 according to Turpin and Lim (2001).

3. Results and discussion

3.1. Evaluation of the meteorological predictions

Meteorology inputs play important roles in the air quality model, which could affect transport, deposition among other processes (Jacob and Winner, 2009). The evaluation of the accuracy of the meteorology inputs to the CMAQ model is a key step to ensure the accuracy of the air quality model predictions. In this study, the observation data is from the Qingpu Supersite. The hourly atmospheric pressure (AP), wind speed (WS), wind direction (WD), relative humidity (RH), and surface temperature (T) are compared with WRF model predictions. Fig. S2 shows the predicted and observed hourly values of these five meteorological factors during the simulation periods at the Qingpu Supersite. The WRF model catches the magnitude and the trends for all factors except missing some peak values of wind speed and relative humidity in winter 2015. Table S1 shows the statistical measures, including the mean observation, mean prediction, mean bias (MB), root mean square error, and normalized mean bias, at 8 monitor sites in the YRD (shown in Fig. 1b and Table S2). In general, the WRF model predictions satisfies the evaluation criteria except for the AP (MB = 1.0) in winter 2015. Simulations of 2016 have better model performance than that of 2015 with the MB values of 0.3, −0.2, −1.78, and −0.27 for AP, WS, RH, and T respectively. Comparing to the previous studies in the YRD region (Chen et al., 2019; Hu et al., 2017b), the overall WRF model performances are considered acceptable to support the CMAQ simulations.

3.2. CMAQ model evaluation

Predicted hourly concentrations of OC, $PM_{2.5}$, and SOA are compared with the observations measured at the Qingpu Supersite in the winter of 2015 and 2016 as shown in Fig. 2. Overall, the CMAQ model successfully captures the hourly variations of these three species. For $PM_{2.5}$, the monthly average concentrations are relatively similar between 2015 and 2016 (96.5 and 99.5 μg/m^3, respectively). In both months, the hourly peak $PM_{2.5}$ concentrations reach >250 μg/m^3.

The CMAQ model slightly under-estimates the $PM_{2.5}$ in 2015 (Mean fraction bias (MFB) = −0.06) while over-estimates the concentrations in 2016 (MFB = 0.19). While the CMAQ model generally agrees with the hourly OC observations, it over-estimates the concentrations in both years as indicated by the positive MFB values (0.19 and 0.37 for 2015 and 2016, respectively). In 2015, the model performs better during the high-OC (>20 μg/m^3) days (January 9–12, 2015), however, it over-estimates the OC in other days. In 2016, the over-estimations of OC become more ubiquitous. Hourly SOA predictions agree well with observations (MFB values are 0.22 and 0.32 for 2015 and 2016 winter, respectively). Similar to OC, in 2015, better model performance occurs in the high-SOA (>30.0 μg/m^3) days, with MFB = 0.22. In 2016, the predicted peak SOA values are relatively close to that of observations except the over-estimation occurred on December 20–21, 2015.In summary, available $PM_{2.5}$, OC, and SOA observations indicate that OC may be slightly over-estimated at the Qingpu Supersite based on the current emission inventory, leading to the SOA over-estimation simultaneously. A more detailed local anthropogenic emission inventory and a higher spatial resolution might be needed to further improve the OC and SOA predictions.

3.3. SOA formation pathways and spatial distribution

Fig. 3 shows predicted average SOA concentrations from different precursors: ARO1 (aromatics with kOH < 5×10^{-4} ppm^{-1} min^{-1}), ARO2 (aromatics with kOH > 5×10^{-4} ppm^{-1} min^{-1}), ALK5 (alkanes with kOH > 1×10^{-4} ppm^{-1} min^{-1}), and primary GLY (glyoxal) and MGLY (methyl-glyoxal) in the YRD of two winter months. For SOA originated from primary emissions of GLY and MGLY, the high SOA regions are located in the

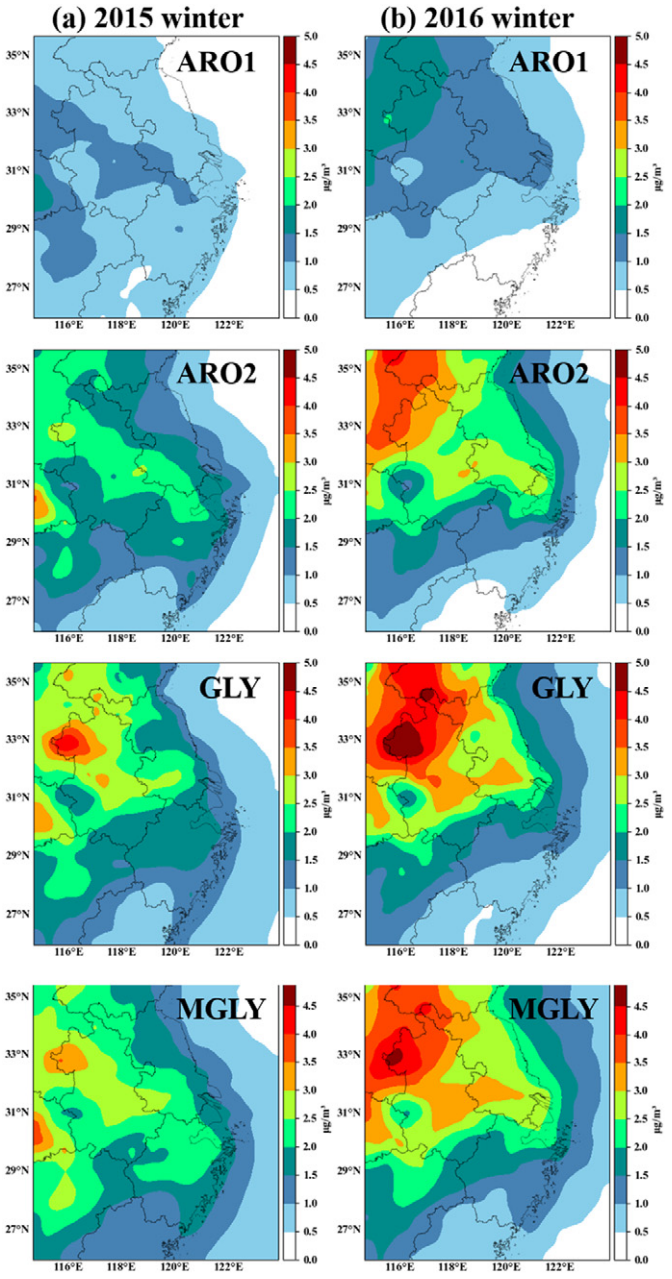

Fig. 3. Spatial distributions by different precursors to SOA in the YRD of 2015 winter and 2016 winter.

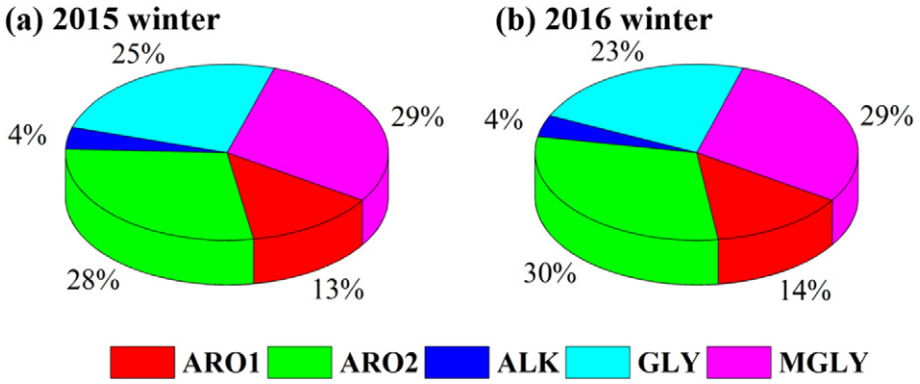

Fig. 4. Average fractional contributions by different precursors to SOA at Qingpu supersite of (a) 2015 winter and (b) 2016 winter. Red block represents ARO1, green block represents ARO2, blue block represents ALK5, cyan block represents GLY, magenta block represents MGLY.

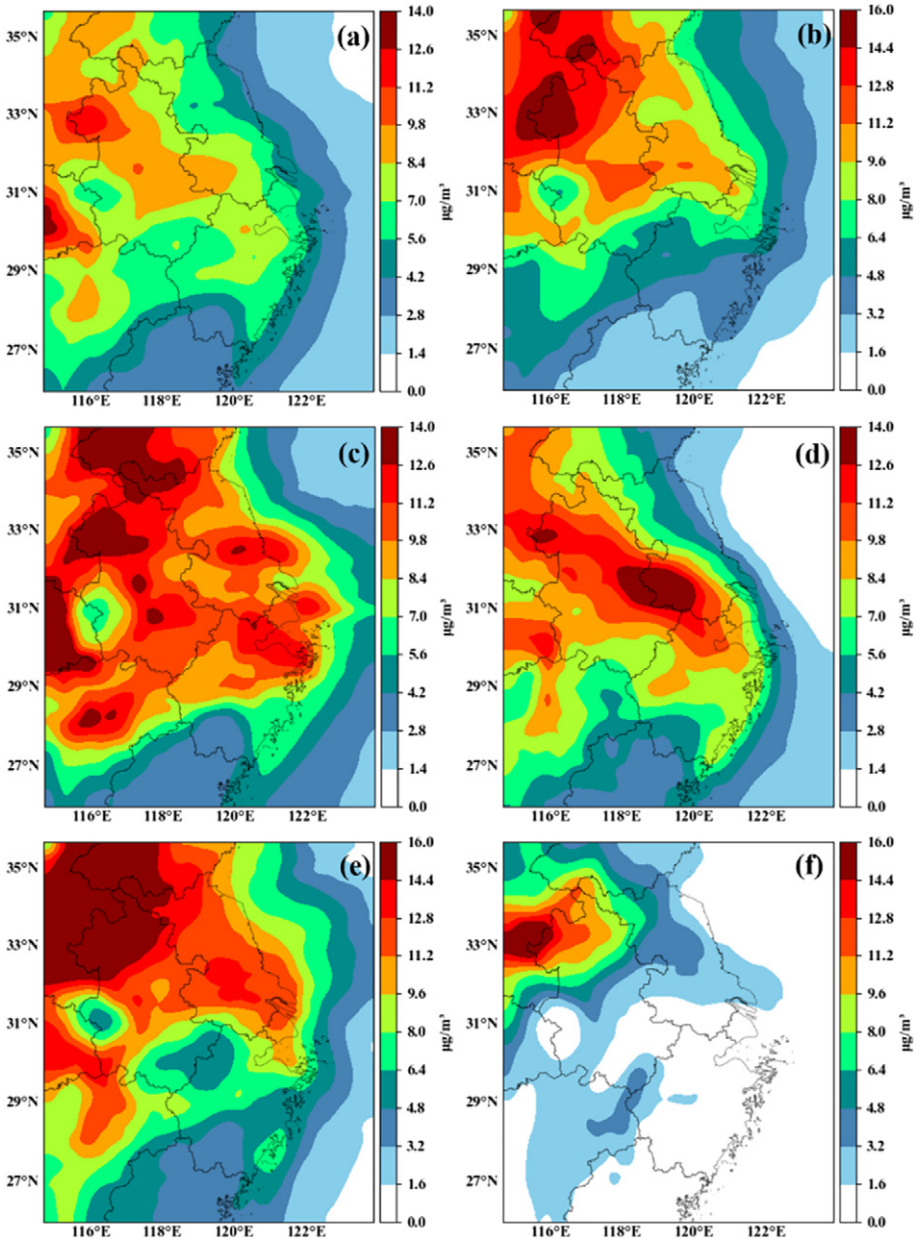

Fig. 5. Predicted SOA regional distributions in the YRD of (a) 2015 winter, (b) 2016 winter, (c) EP1, (d) EP2, (e) EP3, and (f) EP4.

northwest of Anhui and southwest of Shandong with concentrations of ~4.0 μg/m^3 and ~4.5 μg/m^3 in winter 2015 and 2016, respectively. ARO2 also has similar regional contributions to SOA in 2016 with the highest concentrations ~4.0 μg/m^3 in the northwest of Anhui and southwest of Shandong. Fig. 4 illustrates the average fractional contributions of different precursors to SOA in winter 2015 and 2016 at the Qingpu site in Shanghai. GLY and MGLY directly form SOA due to irreversible reactive surface uptake reactions, and can contribute 25%, and 29% in the winter of 2015, and 23%, and 29% in the winter of 2016, respectively. The high SOA concentrations from aromatics oxidation can nerve be forgotten. ARO2 is one of the biggest contributors of both 2015 (28%) and 2016 (30%), and ARO1 can also contribute 13% and 14%, respectively. The fractional contributions from different precursors are similar during the heavy-polluted episodes.

3.4. Averaged SOA source apportionment and regional transport

Fig. 5 shows predicted averaged SOA concentrations in the YRD region of two simulation episodes. Overall, the 2016 winter has higher SOA concentrations than that of 2015 with the highest SOA concentration up to >16.0 μg/m^3, which is mainly due to relatively high predicted SOA concentrations in December 2015 since emissions for January are the same. For both 2015 and 2016 winter, the high SOA regions are located in the northwest of Anhui province (>11 μg/m^3). Also, higher SOA concentrations are observed at east Henan and the conjunction of Jiangsu and Shandong province in winter 2016. At the Qingpu site, SOA concentrations are higher in 2016 (9.6 μg/m^3) than that of 2015 (6.9 μg/m^3) as well. Fig. 6 shows the regional concentrations of averaged SOA attributed to different emission sources in winter 2015 and 2016, respectively. Industry source is the most important emission sector

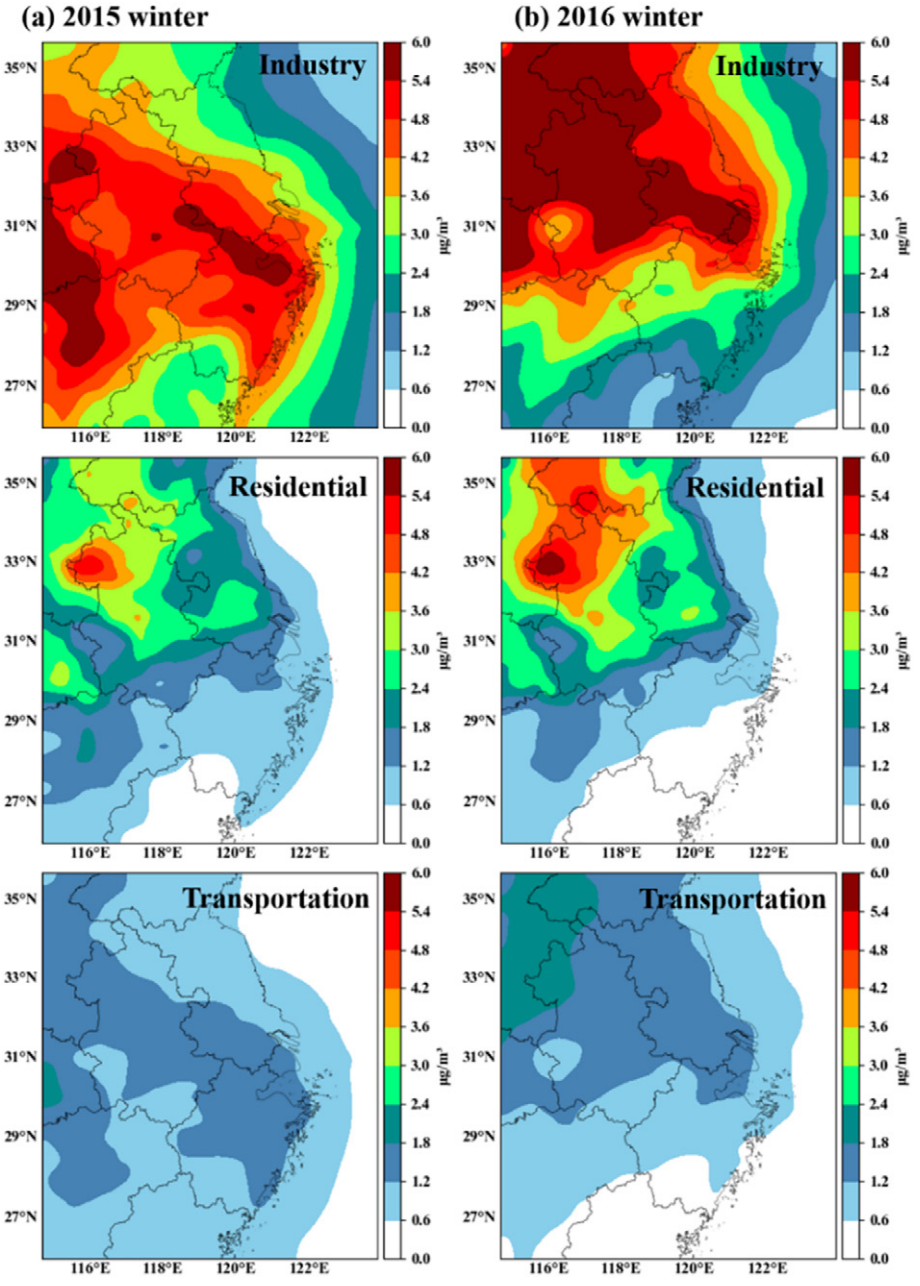

Fig. 6. Spatial distributions by sector (industry, residential and transportation) to SOA in the YRD of 2015 winter and 2016 winter.

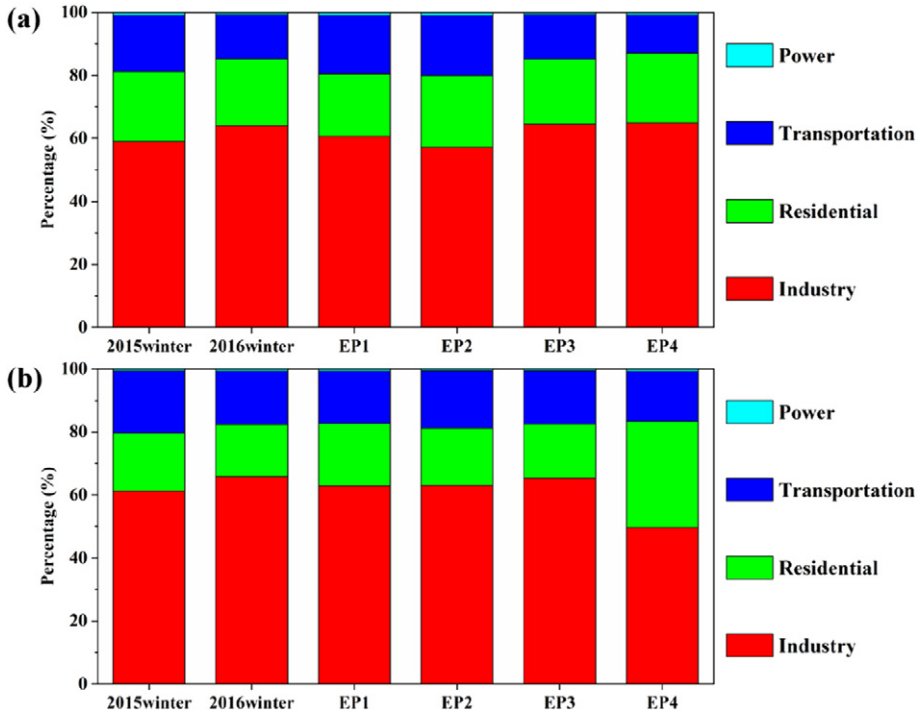

Fig. 7. Average fractional contributions by sector to SOA of (a)the whole YRD and (b) the Qingpu supersite of 2015 winter, 2016 winter, EP1, EP2, EP3 and EP4.

that contributes to the SOA with the higher concentrations (>4 μg/m^3) regions cover vast areas in the YRD. In winter 2016, the SOA from the industry sector is higher than that in 2015. In Anhui, southwest Shandong, and east Henan provinces the maximum concentration is as high as 12 μg/m^3. The residential sector plays an important role in the west Anhui near Henan province with an SOA concentration of over 4 μg/m^3. In winter 2016, the higher SOA concentrations from the residential sector are also observed in south Shandong (up to 5 μg/m^3). In Shanghai, the SOA from the residential sector is only approximately 1.0 μg/m^3 on average. The contributions from the transportation sector are 1.2 μg/m^3 on average. The power sector just contributes to 1% of SOA because of its low VOCs precursor emissions.

Fig. 7 summarizes the source contributions to SOA of the whole YRD and Qingpu supersite. Source contributions of the two places in the two wintertimes are similar. The average contributions of industrial, residential, and transportation sectors in the YRD region during the entire simulation periods are 61%, 22% and 17%, respectively. The industry sector is also the dominant contributor to SOA at the Qingpu supersite with an average contribution of over 60% in both 2015 and 2016 winter. The contributions from transportation and residential sectors are 20% and 19% in winter 2015, and 16% and 17% in winter 2016 respectively. Wang et al. (2018) reported that the transportation sector only contributes 4% SOA in China in wintertime. However, a much higher contribution is observed in this study, suggesting that there can be significant spatial variations in SOA source apportionment. Therefore, SOA control policies should be established based on the local situations. In both years, the contributions from the power sector are relatively small (0.6% and 0.7% for 2015 and 2016, respectively), which is consistent with the previous study (Wang et al., 2018).

In the winter of both 2015 and 2016, the YRD region is under the control of the north and northeast wind (see Fig. S3). Fig. 8 shows the average SOA regional concentrations from different regional sources in the YRD in winter 2015 and 2016. Jiangsu, Shanghai, Zhejiang, Anhui, and Shandong are five important regional contributors to SOA in Shanghai with different regional distributions. For emissions originated from Jiangsu, the high SOA regions are located in northwest Shanghai with concentrations of ~2.0 and ~2.4 μg/m^3 for 2015 and 2016, respectively. Higher SOA concentrations from Jiangsu emissions are observed in 2016 and in most parts of Shanghai contributions to SOA due to emissions from Jiangsu are higher than 1.6 μg/m^3. In 2015, the VOC emissions from Shanghai only have contributed to SOA concentrations within Shanghai, especially in east Shanghai. In winter 2016, the emissions from Shanghai contribute more to SOA in south Jiangsu. The highest SOA concentration from the Shanghai emissions is approximately 1.2 μg/m^3. For the emissions from Zhejiang, the contributions to SOA in Shanghai are mostly in the south part of Shanghai in both years, with concentrations of 1.2 and 2.4 μg/m^3 for 2015 and 2016, respectively. The higher SOA concentrations in central Zhejiang are mainly due to the lower elevation of this region, which prevents the transport of pollutants. Throughout Shanghai, the SOA from Anhui and Shandong sectors are observed with the averaged concentrations of 1.3 μg/m^3 for both 2015 and 2016. Under the impact of the north wind in the wintertime, the SOA from Shandong could cover a vast area in the YRD with the highest areas located in the north part of Jiangsu, with the highest concentrations reaching 2.8 μg/m^3 and 3.6 μg/m^3 in 2015 and 2016, respectively.

Fig. 9a summarizes the fractional contributions from different regions to SOA at Qingpu site. Jiangsu, Zhejiang, Shanghai, Shangdong, Anhui are the five major regional contributors to SOA in Shanghai with a total contribution of over 75%. Jiangsu is the most important contributor (31% on average) followed by Zhejiang (19%). In 2016, contributions from the Zhejiang and Shanghai increase to 22% and 16% from 15% and 9% respectively in 2015. In addition, contributions from emission regions further away, such as Hebei and Beijing, also observed in Shanghai. Fig. 10 shows the time series contributions. On January 11, and 24–25, 2015, and January 3–4, 2016, contributions from Zhejiang see a significant increase. That is mainly caused by the wind direction changes from northeast to westsouth in these days (see Fig. S2). Therefore, changing wind directions can absolutely effect the regional transport results.

Considering the synergistic impacts from both emissions and regional sources, the industry from Jiangsu, industry from Zhejiang, and

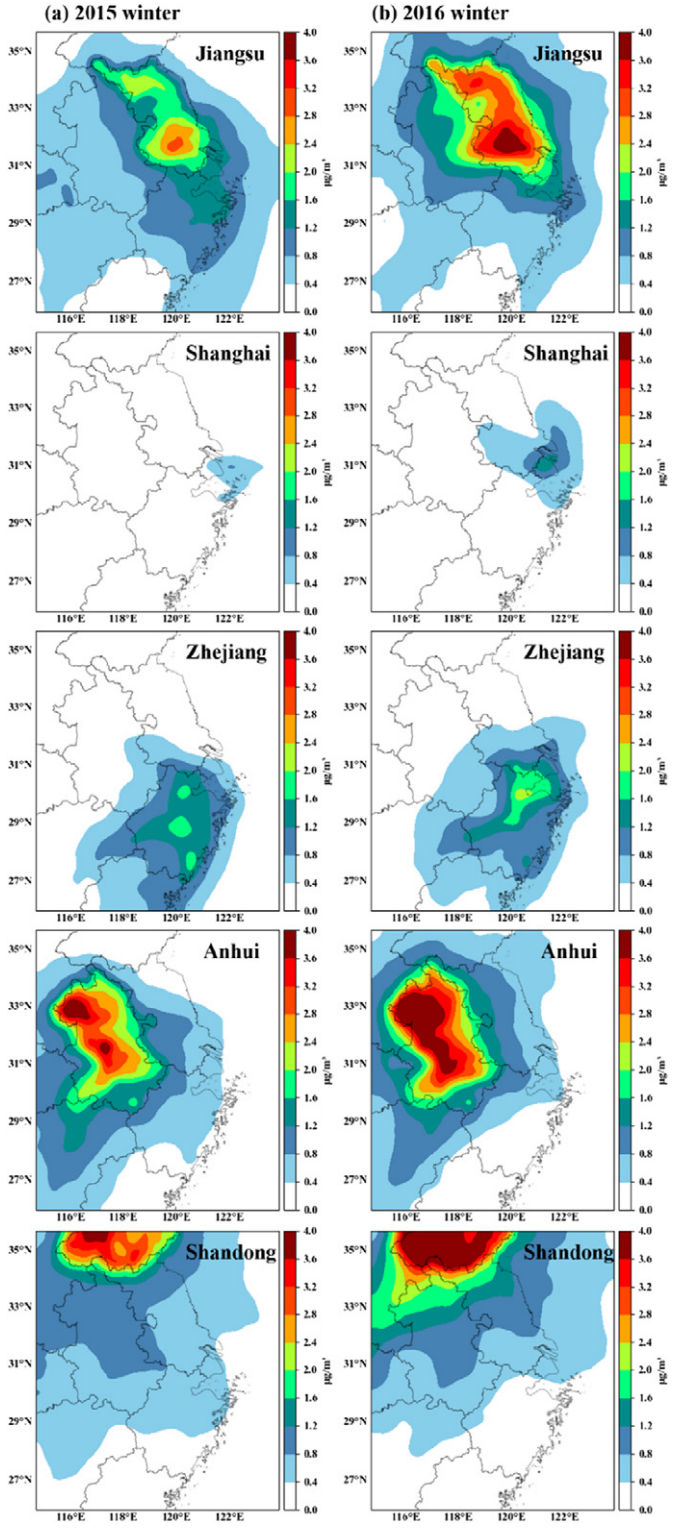

Fig. 8. Spatial distributions by region (Jiangsu, Shanghai, Zhejiang, Anhui and Shandong) to SOA in the YRD of 2015 winter and 2016 winter.

transportation from Jiangsu are the most important contributors to SOA in Shanghai in 2015 (see Fig. 9b). However, the industry from Jiangsu, industry from Zhejiang, and industry from Shanghai become in 2016 with a total contribution of over 40%. Although the prevailing wind directions are north in wintertime in Shanghai, Zhejiang is still a significant contributor to SOA, especially for the industrial emissions. In addition, super-regional sources (others in Fig. 9b) contribute 24% and 20% to SOA in Shanghai for 2015 and 2016, respectively, indicating the regional transport impacts should be included in the local SOA control policy.

3.5. SOA source apportionment and regional transport under haze and clean days

To investigate the source contributions to SOA and establish effective SOA control in Shanghai, the simulation periods are further split into 4 episodes as shown in Table S3. EP1 ($PM_{2.5}$: 138.90 μg/m^3) and EP2 ($PM_{2.5}$: 118.66 μg/m^3) are considered as the heavy-pollution episodes in 2015. EP3 ($PM_{2.5}$: 109.42 μg/m^3) is a heavy-pollution episode in 2016, and EP4 is the clean episode in 2016 (47.41 μg/m^3). The higher wind speed (up to 4 m/s in most of the two episodes; see Figs. S2 and S3) are favorable for the dilution of the SOA precursors. However, relatively low solar radiation in EP4 (Fig. S4) can further lead to a significant decrease in SOA concentrations. In EP4, the predicted SOA concentration is only 0.68 μg/m^3 on average, while it is 10.21 μg/m^3, 9.46 μg/m^3, and 12.48 μg/m^3 for EP1, EP2, and EP3, respectively. Simultaneously, the SOA fraction in total $PM_{2.5}$ (SOA/$PM_{2.5}$) drops sharply in the EP4. In the heavy-polluted episodes (EP1, EP2, and EP3), the SOA/$PM_{2.5}$ values could reach to >30% in Shanghai (see Fig. S5). In contrast, this fraction is <10% in the whole EP4. In the EP1, the higher SOA concentrations regions (>8 μg/m^3) are located throughout the domain except for the south part of Zhejiang. However, these higher concentrations regions only cover the southwest Jiangsu, west Shanghai, and north Zhejiang. In the EP3, peak SOA concentrations are in the west north of the YRD. In Shanghai, higher SOA concentrations (9–12 μg/m^3) occur during EP1 and EP3. The peak hourly concentration of SOA in Shanghai can be as high as 31 μg/m^3 (EP2) and 48 μg/m^3 (EP3) in 2015 and 2016, respectively. The fractional contributions from emission sources are similar during the heavy-polluted episodes (Fig. S6), while, an increasing contribution from the transportation is observed in the clean episode (see Fig. 7a). During the clean days, the contribution from the transportation sector increases from 18% to 33%. Jiangsu, Zhejiang, Shanghai, and Anhui are four major contributors to SOA in Shanghai during the heavy-polluted episodes with the averaged contributions of 25%, 24%, 10%, and 8% respectively (Fig. 9a and Fig. S7). In 2016, Zhejiang is the most important contributor to SOA in Shanghai (EP3) instead of Jiangsu in 2015, suggesting that the regional control policy should be considered rather than the local one in the VOCs and SOA reduction. In the clean days, the contributions from the downwind regional sectors such as Zhejiang are further reduced due to the higher wind speed. A significant reduce (from 8% to 1%) of Anhui sector also occurs during the clean days. The industry emissions from the key areas (Jiangsu, Zhejiang, and Shanghai) are the most contributors to the SOA in Shanghai during the heavy-polluted episodes (see Fig. 9b and Fig. S8). Except for the EP3, the transportation sector from Jiangsu plays an important role in the SOA in Shanghai during both heavy-polluted and clean episode with the averaged contribution of 28%. The SOA precursors from the transportation sector should be considered in the control policy as well.

4. Conclusion

In this study, we applied the source-oriented treatment in CMAQ coupled with the modified SAPRC-11 chemical mechanism and relevant SOA module to conduct the source apportionment and regional transport of SOA in the YRD, with a monthly average of 6.9 and 9.6 μg/m^3 for 2015 and 2016 winter respectively, mainly due to industry source, the most important emission sector that contribute to the SOA (over 60%) in both two winters. Fractional contributions from emission sources in the wintertime are similar to which in the three heavy-polluted episodes, indicating that cutting down industry emissions would efficiently reduce the overall SOA pollution. Regional transport

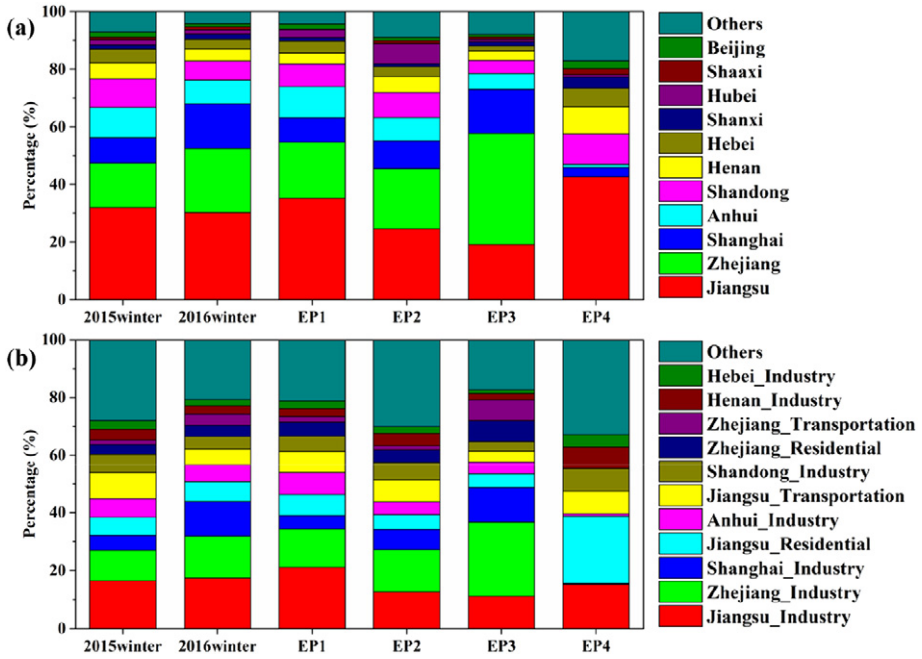

Fig. 9. Temporal variation in the contributions by region (a) and regional sectors (b) to SOA at Qingpu supersite of 2015 winter, 2016 winter, EP1, EP2, EP3 and EP4.

results show that Jiangsu, Zhejiang, Shanghai, Anhui and Shandong are five major contributors to SOA. However, Zhejiang is the most important contributor to SOA in EP3 of 2016 winter (35%) instead of Jiangsu in 2015 winter (32%, averagely), suggesting that the regional control policy also should be considered in the VOCs and SOA reduction. Further study shows that the industrial emissions of Jiangsu, Zhejiang, and Shanghai are the most contributors to the SOA during the heavy-polluted episodes. Therefore, the most cost-effective SOA reduction strategy is to impose restrictions on industry sources from those key areas. The government can control the SOA pollution during the heavy-polluted episodes by cutting the industrial emissions in Jiangsu, Zhejiang, and Shanghai. And it should be noted that the quantity of SOA source apportionment and regional transport in this study is based on the Qingpu supersite. SOA modeling studies with a higher solution in different places can be conducted to compare the regional features of SOA formation.

Declaration of competing interest

We declare that that we have no known competing financial interests or personal relationships that could have appeared to influence the work reported in this paper.

Acknowledgments

This work was supported by the National Key Research and Development Program of China (2016 YFC0208700), the National Natural Science Foundation of China (21607100). This work was also supported

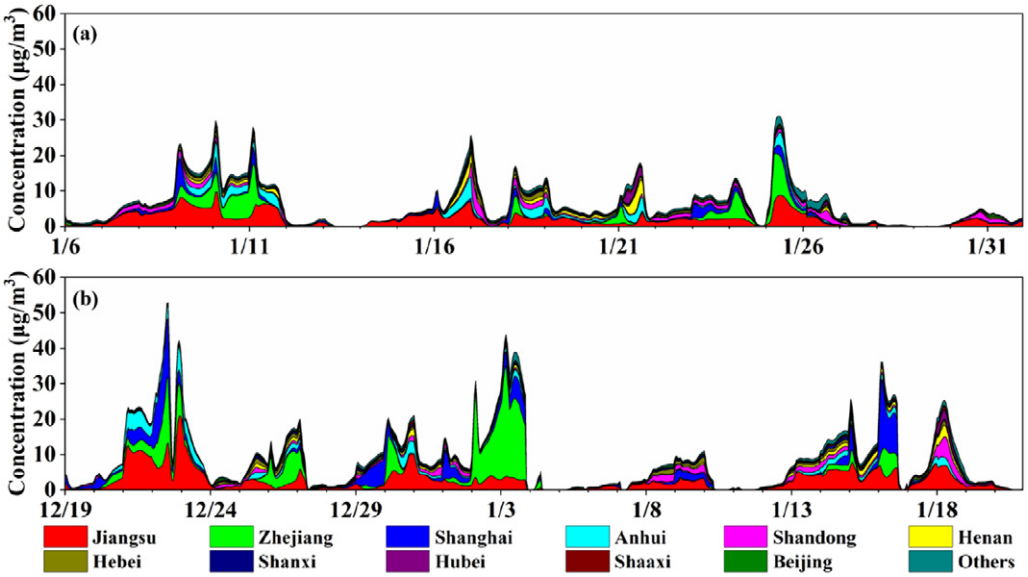

Fig. 10. Temporal variation in the contributions by region to SOA at Qingpu supersite of (a) 2015 winter and (b) 2016 winter.

by the Center for High Performance Computing in Shanghai Jiao Tong University

Appendix A. Supplementary data

Supplementary data to this article can be found online at https://doi.org/10.1016/j.scitotenv.2019.135620.

References

Bae, M., Schauer J., J., DeMinter T., J., Turner R., J., Smith, D., Cary A., R., et al., 2004. Validation of a semi-continuous instrument for elemental carbon and organic carbon using a thermal-optical method. Atmospheric Environment 38 (18), 2885–2893.

Byun, D., Schere, K.L., 2006. Review of the governing equations, computational algorithms, and other components of the models-3 community multiscale air quality (CMAQ) modeling system. Appl. Mech. Rev. 59, 51–77.

Cao, J.J., Lee, S.C., Ho, K.F., Zou, S.C., Fung, K., Li, Y., et al., 2004. Spatial and seasonal variations of atmospheric organic carbon and elemental carbon in Pearl River Delta Region, China. Atmos. Environ. 38, 4447–4456.

Carter, W.P.L., Heo, G., 2013. Development of revised SAPRC aromatics mechanisms. Atmos. Environ. 77, 404–414.

Castro, L.M., Pio, C.A., Harrison, R.M., Smith, D.J.T., 1999. Carbonaceous aerosol in urban and rural European atmospheres: estimation of secondary organic carbon concentrations. Atmos. Environ. 33, 2771–2781.

Chen, D.S., Tian, X.L., Lang, J.L., Zhou, Y., Li, Y., Guo, X.R., et al., 2019. The impact of ship emissions on PM2.5 and the deposition of nitrogen and sulfur in Yangtze River Delta, China. Sci. Total Environ. 649, 1609–1619.

Crippa, M., Canonaco, F., Lanz, V.A., Äijälä, M., Allan, J.D., Carbone, S., et al., 2014. Organic aerosol components derived from 25 AMS data sets across Europe using a consistent ME-2 based source apportionment approach. Atmos. Chem. Phys. 14, 6159–6176.

Hu, J., Chen, J., Ying, Q., Zhang, H., 2016. One-year simulation of ozone and particulate matter in China using WRF/CMAQ modeling system. Atmos. Chem. Phys. 16, 10333–10350.

Hu, J., Li, X., Huang, L., Ying, Q., Zhang, Q., Zhao, B., et al., 2017a. Ensemble prediction of air quality using the WRF/CMAQ model system for health effect studies in China. Atmos. Chem. Phys. 17, 13103–13118.

Hu, J., Wang, P., Ying, Q., Zhang, H., Chen, J., Ge, X., et al., 2017b. Modeling biogenic and anthropogenic secondary organic aerosol in China. Atmos. Chem. Phys. 17, 77–92.

Huang, J., Pan, X., Guo, X., Li, G., 2018. Health impact of China's air pollution prevention and control action plan: an analysis of national air quality monitoring and mortality data. The Lancet Planetary Health 2, e313–e323.

Jacob, D.J., Winner, D.A., 2009. Effect of climate change on air quality. Atmos. Environ. 43, 51–63.

Jiang, F., Liu, Q., Huang, X., Wang, T., Zhuang, B., Xie, M., 2012. Regional modeling of secondary organic aerosol over China using WRF/Chem. J. Aerosol Sci. 43, 57–73.

Jimenez, J.L., Canagaratna, M.R., Donahue, N.M., Prevot, A.S.H., Zhang, Q., 2009. Evolution of organic aerosols in the atmosphere. Science 326, 1525–1529.

Kang, M., Ren, L., Ren, H., Zhao, Y., Kawamura, K., Zhang, H., et al., 2018. Primary biogenic and anthropogenic sources of organic aerosols in Beijing, China: insights from saccharides and n-alkanes. Environ. Pollut. 243, 1579–1587.

Kleindienst, T.E., Jaoui, M., Lewandowski, M., Offenberg, J.H., Lewis, C.W., Bhave, P.V., et al., 2007. Estimates of the contributions of biogenic and anthropogenic hydrocarbons to secondary organic aerosol at a southeastern US location. Atmos. Environ. 41, 8288–8300.

Li, M., Zhang, Q., Zheng, B., Tong, D., Lei, Y., Liu, F., et al., 2019. Persistent growth of anthropogenic non-methane volatile organic compound (NMVOC) emissions in China during 1990–2017: drivers, speciation and ozone formation potential. Atmos. Chem. Phys. 19, 8897–8913.

Lin, J., An, J., Qu, Y., Chen, Y., Li, Y., Tang, Y., et al., 2016. Local and distant source contributions to secondary organic aerosol in the Beijing urban area in summer. Atmos. Environ. 124, 176–185.

Liu, Y., Li, L., An, J.Y., Huang, L., Yan, R.S., Huang, C., et al., 2018. Estimation of biogenic VOC emissions and its impact on ozone formation over the Yangtze River Delta region, China. Atmos. Environ. 186, 113–128.

Turpin, B.J., Lim, H.J., 2001. Species contributions to PM2.5 mass concentrations: revisiting common assumptions for estimating organic mass. Aerosol Sci. Technol. 35, 602–610.

Wang, P., Ying, Q., Zhang, H., Hu, J., Lin, Y., Mao, H., 2018. Source apportionment of secondary organic aerosol in China using a regional source-oriented chemical transport model and two emission inventories. Environ. Pollut. 237, 756–766.

Wei, X.Y., Liu, M., Yang, J., Du, W.N., Sun, X., Huang, Y.P., et al., 2019. Characterization of PM2.5-bound PAHs and carbonaceous aerosols during three-month severe haze episode in Shanghai, China: chemical composition, source apportionment and long-range transportation. Atmos. Environ. 203, 1–9.

Wu, K., Yang, X., Chen, D., Gu, S., Lu, Y., Jiang, Q., et al., 2019. Estimation of biogenic VOC emissions and their corresponding impact on ozone and secondary organic aerosol formation in China. Atmos. Res. 231, 1–11.

Ying, Q., Krishnan, A., 2010. Source contributions of volatile organic compounds to ozone formation in southeast Texas. J. Geophys. Res. 115.

Ying, Q., Li, J., Kota, S.H., 2015. Significant contributions of isoprene to summertime secondary organic aerosol in eastern United States. Environ. Sci. Technol. 49, 7834–7842.

Zhang, H., Ying, Q., 2011a. Contributions of local and regional sources of NOx to ozone concentrations in Southeast Texas. Atmos. Environ. 45, 2877–2887.

Zhang, H., Ying, Q., 2011b. Secondary organic aerosol formation and source apportionment in Southeast Texas. Atmos. Environ. 45, 3217–3227.

Zhang, H., Li, J., Ying, Q., Yu, J.Z., Wu, D., Cheng, Y., et al., 2012. Source apportionment of PM2.5 nitrate and sulfate in China using a source-oriented chemical transport model. Atmos. Environ. 62, 228–242.

Zhu, Y., Yang, L., Kawamura, K., Chen, J., Ono, K., Wang, X., et al., 2017. Contributions and source identification of biogenic and anthropogenic hydrocarbons to secondary organic aerosols at Mt. Tai in 2014. Environ. Pollut. 220, 863–872.